

Review

Nucleation and Growth of an Ensemble of Crystals during the Intermediate Stage of a Phase Transition in Metastable Liquids

Liubov V. Toropova ^{1,2,*} , Eugeny V. Makoveeva ³ , Sergei I. Osipov ⁴, Alexey P. Malygin ⁴, Yang Yang ⁵ 
and Dmitri V. Alexandrov ³ 

¹ Laboratory of Mathematical Modeling of Physical and Chemical Processes in Multiphase Media, Department of Theoretical and Mathematical Physics, Ural Federal University, Lenin Ave., 51, 620000 Ekaterinburg, Russia

² Otto-Schott-Institut für Materialforschung, Friedrich-Schiller-Universität-Jena, 07743 Jena, Germany

³ Laboratory of Multi-Scale Mathematical Modeling, Department of Theoretical and Mathematical Physics, Ural Federal University, Lenin Ave., 51, 620000 Ekaterinburg, Russia; e.v.makoveeva@urfu.ru (E.V.M.); dmitri.alexandrov@urfu.ru (D.V.A.)

⁴ Institute of Natural Sciences and Mathematics, Ural Federal University, Lenin Ave., 51, 620000 Ekaterinburg, Russia; sergei.osipov@urfu.ru (S.I.O.); alexey.malygin@urfu.ru (A.P.M.)

⁵ Key Laboratory of Polar Materials and Devices and Physics Department, East China Normal University, Shanghai 200241, China; yyang@phy.ecnu.edu.cn

* Correspondence: l.v.toropova@urfu.ru

Abstract: In this paper, an analytical method of solving the integro-differential system of kinetic and balance equations describing the evolution of an ensemble of crystals during the intermediate phase of the bulk crystallization process is described. The theory is developed for kinetic equations of the first- and second order corresponding to the absence and presence of fluctuations in particle growth rates. The crystal-size distribution function as well as the dynamics of metastability reduction in a supercooled melt (supersaturated solution) are analytically found using the saddle-point and the Laplace transform methods. The theory enables us to obtain the crystal-size distribution function that establishes in a supercooled (supersaturated) liquid at the beginning of the final stage of a phase transformation process when Ostwald ripening, coagulation and fragmentation of crystals are able to occur.

Keywords: nucleation; crystal growth; phase transformation; supercooled liquid; crystal-size distribution



Citation: Toropova, L.V.; Makoveeva, E.V.; Osipov, S.I.; Malygin, A.P.; Yang, Y.; Alexandrov, D.V. Nucleation and Growth of an Ensemble of Crystals during the Intermediate Stage of a Phase Transition in Metastable Liquids. *Crystals* **2022**, *12*, 895. <https://doi.org/10.3390/cryst12070895>

Academic Editor: Sławomir Grabowski

Received: 6 June 2022
Accepted: 22 June 2022
Published: 24 June 2022

Publisher's Note: MDPI stays neutral with regard to jurisdictional claims in published maps and institutional affiliations.



Copyright: © 2022 by the authors. Licensee MDPI, Basel, Switzerland. This article is an open access article distributed under the terms and conditions of the Creative Commons Attribution (CC BY) license (<https://creativecommons.org/licenses/by/4.0/>).

1. Introduction

The phase transformations from a metastable to a thermodynamically stable state are accompanied by the growth of new phase particles on microscopic inclusions or impurities. In the early stages of a phase transformation, the evolution of nuclei can be considered independently of each other, whereas in the later stages of the process it is necessary to take into account the interaction between growing crystallites, which affects the degree of liquid metastability (its supercooling or supersaturation) [1–5]. The dynamic process of evolution of a metastable zone filled with the crystals at all stages of the phase transition is important from the theoretical and applied points of view. In particular, this applies to crystallization from supercooled melts or supersaturated solutions, where the phase transition is maintained by fluctuations in the growth rates of particles, and the contribution from impurity (representing nucleation sites) is rather small [6,7]. Note that crystal nucleation and growth processes control the size distributions obtained in laboratory and industrial crystallizers [8–13]. As this occurs, the growth rate of solid phase particles also plays a key role in the evolution of the metastable system and, thus, in the physico-chemical properties of the produced materials [14,15].

Generally speaking, the process of bulk phase transformation from a supercooled melt or supersaturated solution may be described by four main stages [16,17]. The supercooled

(supersaturated) state is established in the preliminary stage. Then, in the initial stage, the formation of new phase nuclei occurs (in a heterogeneous or homogeneous manner). Next, nucleation, crystal growth, and partial supercooling (or desupersaturation) occur in the intermediate stage. A final stage describes the relaxation processes of Ostwald ripening, coagulation, and particle fragmentation [18]. The study of the initial stages of the phase transition is generally based on kinetic nucleation theory and on the assumption that the growth of individual particles is independent [19–21]. The final stage of a phase transformation is analyzed according to the Lifshitz-Slyozov theory, which is based on the assumptions that no particles of a new phase appear and that large crystals grow at the expense of small ones [22–28].

The present paper is focused on the study of the intermediate stage when the processes of nucleation of the new phase elements and the growth of already existing crystals are of same importance. The general theory of this stage is incomplete, however the intermediate stage often takes most of the time of the whole phase transition process. This is caused, in particular, since the corresponding mathematical model of the process is integro-differential, and some of the boundary conditions are put on the moving growth boundaries. Note that complete information on the dynamics of metastability removal and evolution of the new phase may be derived by analyzing just this stage. The absence of universal methods for solving the integrodifferential equations is the reason why the dynamics of desupercooling (or desupersaturation) is completely ignored in several evolutionary models [29,30]. Note that the necessity of simultaneous accounting for the processes of nucleation and growth of a new phase is described, for example, in Refs. [31,32]. Nevertheless, many models are based on stationary approximations (see, e.g., [33,34]), which may occur only at the very initial stages or in the case of particular system parameters.

The earliest attempt to overcome the above described difficulties of formulating and solving a mathematical model was undertaken in Ref. [35] using the saddle-point method of calculating a Laplace-type integral. A similar approach was then used to solve problems about the evolution of aggregates in magnetic fluids and metastable colloids [36,37]. The approach and solutions [35] were then applied to describe protein crystallization [38] and to verify von Weimarn theory describing the average size of crystals [39]. It is important to note that the analytical solutions were obtained only for the main contribution to the Laplace integral [35]. This contribution leads to the zero-order approximation of the Laplace integral in the neighborhood of the saddle point. In this case, the dimensionless Gibbs number p included in the nucleation frequency $I = I_* \exp(-p/v^2)$ formally tends to infinity, where v and I_* denote the dimensionless supercooling/supersaturation and pre-exponential factor. Since p varies from $\sim 10^{-1}$ to $\sim 10^3$ for real supercooled melts or supersaturated solutions, the theory of Ref. [35] must be developed to describe such systems. It is also important to note that even in the case of sufficiently large $p \sim 10^2 - 10^3$ the zero-order solution of Ref. [35] differs significantly from the complete solution containing the following terms. Here we develop the nucleation and growth theory at the intermediate stage with allowance for additional terms to the aforementioned zero-order solution and possible fluctuations in crystal growth rates.

2. The Model of Nucleation and Crystal Growth

The molecular-kinetic theory is based on the assumption that micronuclei of a new phase may form as a result of density fluctuations in metastable melts or solutions [19,20,40–42]. If the characteristic size of such nuclei exceeds some critical value r_* , they are able to grow further and it will take work to form a new spherical particle of radius r in a one-component system

$$Y(r) = 4\pi r^2 \gamma_i - \frac{4}{3} \pi r^3 \rho_s (\mu_l - \mu_s), \quad (1)$$

where ρ_s is the solid phase density, γ_i is the surface tension, μ_s and μ_l are the chemical potentials of the solid and liquid phases, respectively, and $\mu_l > \mu_s$ for a metastable melt. However, the critical radius r_* of a particle can be achieved when $Y(r)$ reaches a maximum.

In this case, particles with radii $r = r_*$ are unstable, and the work Y_* of their formation can be written as

$$Y_* = \frac{16\pi\gamma_i^3}{3\rho_s^2(\mu_l - \mu_s)^2}. \quad (2)$$

The chemical potential difference may be calculated using the Gibbs-Helmholtz equation and has a form [43]

$$\mu_l - \mu_s = \frac{L\Delta T}{T_p}, \quad \Delta T = T_p - T_l, \quad (3)$$

where L represents the latent heat of the phase transition, and T_p and T_l are the phase transition and melt temperatures, respectively. Nucleation of a new phase occurs if the energy barrier Y_* that prevents nucleation is overcome. In this case, the nucleation frequency can be represented as an exponential function of the energy barrier height [16,42,44]. Thus, we obtain

$$I = I_* \exp\left(\frac{-Y_*}{k_B T_l}\right) = I_* \exp\left(\frac{-16\pi\gamma_i^3 T_p^2}{3\rho_s^2 L^2 \Delta T^2 k_B T_l}\right), \quad (4)$$

where k_B stands for the Boltzmann constant. The pre-exponential factor I_* weakly depends on supercooling/supersaturation (metastability degree) [20,40,41,45] and can be a function of r [33]. However, in the present paper I_* is assumed to be a constant, because the nucleation frequency is included only in the boundary condition at $r = r_*$. Considering $\Delta T \ll T_p$, expression (4) can be rewritten as

$$I = I_* \exp\left(\frac{-16\pi\gamma_i^3 T_p}{3\rho_s^2 L^2 \Delta T^2 k_B}\right). \quad (5)$$

The model is applicable for single-component melts and should be modified for binary systems. In that case, the phase transition temperature T_p must be replaced by the function $T_p(C_l)$, as it depends on the impurity concentration C_l . Equation (5) can be rewritten as

$$I = I_* \exp\left[\frac{-p}{(\Delta T/\Delta T_0)^2}\right], \quad p = \frac{16\pi\gamma_i^3 T_p}{3\rho_s^2 L^2 \Delta T_0^2 k_B}, \quad (6)$$

where ΔT_0 is the characteristic supercooling. Expression (6) defines the nucleation frequency as a function of dimensionless supercooling $v = \frac{\Delta T}{\Delta T_0}$, and in the case of supersaturated solutions has a form [46]

$$I = I_* \exp\left[\frac{-p}{\ln^2(C_l/C_p)}\right], \quad p = \frac{16\pi\gamma_i^3 M_s^2}{3\rho_s^2 R_g^2 T_s^3 k_B}. \quad (7)$$

Here C_p is the supersaturation concentration, M_s is the molecular weight, R_g is the universal gas constant, and T_s is the solution temperature.

Further, we will use a quasi-stationary approximation to solve a Stefan-type problem with a moving phase transition boundary, which occurs as a result of nucleus growth. The temperature/concentration field T around the growing spherical particle and a growth rate $\frac{dr}{d\tau}$ take a form

$$\begin{aligned} \nabla^2 T = 0, \quad \rho > r(\tau), \quad \frac{dr}{d\tau} = -\frac{\lambda_l}{\rho_s L} \frac{\partial T}{\partial \rho} = \beta_*(T_p - T), \\ \rho = r(\tau), \quad \rho/r(\tau) \gg 1, \quad T \rightarrow T_l, \end{aligned} \quad (8)$$

where ρ represents the spherical coordinate, λ_l is the thermal conductivity coefficient of the liquid phase, β_* is the kinematic parameter, and τ stands for time. The solution of Equation (8) defines the particle growth rate as

$$\frac{dr}{d\tau} = \frac{\beta_* \Delta T}{1 + \beta_* q r}, \quad q = \frac{\rho_s L}{\lambda_l}. \quad (9)$$

Expression (9) represents the growth rate as a linear function of supercooling that has two regimes. When the crystal size is small, $r \ll (\beta_* q)^{-1}$, growth regime is called kinetic, since it is entirely determined by surface processes. The other regime occurs when the crystals significantly exceed the value of $(\beta_* q)^{-1}$, and the growth rate is controlled by heat dissipation velocity. In the case of liquid solutions, Equation (9) can be rewritten as [47]

$$\frac{dr}{d\tau} = \frac{\beta_* \Delta C}{1 + \beta_* q_C r}, \quad q_C = \frac{C_p (k_0 - 1)}{D}, \quad (10)$$

where k_0 is the partition coefficient, D and ΔC represent the diffusion coefficient and the liquid supersaturation, respectively.

Next, consider a system of spherical solid crystals in a macroscopically homogeneous one-component supercooled (supersaturated) system. The evolution of the system can be described by the Fokker-Planck type kinetic equation. Neglecting random fluctuations in the crystal growth rate and considering a temperature distribution in the system as homogeneous, we get

$$\frac{\partial \phi}{\partial \tau} + \frac{\partial}{\partial r} \left(\frac{dr}{d\tau} \phi \right) = 0, \quad r > r_*, \quad (11)$$

$$\rho_m C_m \frac{d\Delta T}{d\tau} = -4\pi \rho_s L \int_{r_*}^{\infty} r^2 \frac{dr}{d\tau} \phi dr, \quad (12)$$

where ϕ is a number size density, C_m and ρ_m are heat capacity and constant density of a melt, respectively. We also suppose that the liquid instantaneously cools down below the crystallization temperature by ΔT_0 at the initial moment. The boundary conditions for Equations (11) and (12) can be written as

$$\tau = 0, \quad \Delta T = \Delta T_0, \quad \phi = 0, \quad (13)$$

$$r = r_*, \quad \frac{dr}{d\tau} \phi = I(\Delta T). \quad (14)$$

Expressions (4)–(7) and (9)–(14) represent a complete system of equations describing the intermediate stage of bulk phase transitions.

3. Kinetics of Supercooling (Supersaturation) Removal

Let us introduce the following dimensionless parameters and variables

$$\zeta = \frac{r}{l_0}, \quad t = \frac{\tau}{\tau_0}, \quad v = \frac{\Delta T}{\Delta T_0}, \quad \Phi = l_0^4 \phi, \quad (15)$$

$$\tau_0 = \left(\beta_*^3 \Delta T_0^3 I_0 \right)^{-1/4}, \quad l_0 = (\beta_* \Delta T_0)^{1/4} I_0^{-1/4}, \quad \alpha_* = \frac{\beta_* \rho_s L l_0}{\lambda_l}, \quad B_1 = \frac{4\pi \rho_s L}{\rho_m C_m \Delta T_0}, \quad (16)$$

where $I_0 = I(\Delta T_0)$. Rewriting the statement of the problem ($r_* \rightarrow 0$) in dimensionless variables (16), we arrive at

$$\frac{\partial \Phi}{\partial t} + v \frac{\partial}{\partial \zeta} \left(\frac{\Phi}{1 + \alpha_* \zeta} \right) = 0, \quad \zeta > 0, \quad (17)$$

$$\frac{dv}{dt} = -B_1 v \int_0^\infty \frac{\zeta^2 \Phi(t, \zeta)}{1 + \alpha_* \zeta} d\zeta, \quad (18)$$

$$\Phi = 0, \quad t = 0, \quad v = 1, \quad (19)$$

$$\Phi = \frac{1}{v} \exp[pg(v)], \quad \zeta = 0. \quad (20)$$

Note that the dimensionless model (17)–(20) defines an intermediate stage of phase transitions both for supercooled melts and supersaturated solutions. The function $g(v)$ determines the kinetic law of the process in Equation (20) that can be used for both homogeneous and heterogeneous nucleation [48].

In the case of supercooled melt (lower index “sm”) and Weber-Volmer-Frenkel-Zel’dovich kinetics (WVZFZ), we obtain the function $g(v)$ from Equation (6) as

$$g(v) = g_{sm} = 1 - v^{-2}. \quad (21)$$

Using the empirical law $I = I_*(\Delta T)^p$ for the nucleation frequency, (see [49]), we have

$$g(v) = g_{sm} = \ln v. \quad (22)$$

In the case a supersaturated solution (lower index “ss”), v represents dimensionless supersaturation, and dimensionless parameters can be defined as

$$v = \frac{\Delta C}{\Delta C_0}, \quad \alpha_* = \frac{\beta_* C_p l_0}{D}, \quad B_1 = \frac{4\pi C_p}{\Delta C_0}, \quad \tau_0 = (\beta_*^3 \Delta C_0^3 I_0)^{-1/4}, \quad l_0 = (\beta_* \Delta C_0)^{1/4} I_0^{-1/4}, \quad (23)$$

where ΔC_0 is the initial supersaturation.

Further, for a supersaturated solution with WVZFZ kinetics, we obtain from expression (7)

$$g(v) = g_{ss} = \ln^{-2}\left(1 + \frac{1}{v_p}\right) - \ln^{-2}\left(1 + \frac{v}{v_p}\right), \quad (24)$$

where $v_p = \frac{C_p}{\Delta C_0}$.

In the case of a supersaturated solution with Meirs kinetics $I = I_*(\Delta C)^p$ [44], we have

$$g(v) = g_{ss} = \ln v. \quad (25)$$

The kinetics of metastability removal is described by the nonlinear integro-differential Equations (17) and (18). The analytical solution of the model is obtained from the saddle-point method for calculating a Laplace-type integral [50,51]. The solution to Equation (17) with boundary and initial conditions (19) and (20) is given by

$$\Phi(t, \zeta) = (1 + \alpha_* \zeta) \varphi(\xi(t) - \eta(\zeta)) \text{Heav}(\xi(t) - \eta(\zeta)), \quad (26)$$

where

$$\varphi(\xi(t)) = \frac{1}{v(t)} \exp[pg(v(t))], \quad \xi(t) = \int_0^t v(t) dt, \quad \eta(\zeta) = \int_0^\zeta (1 + \alpha_* \zeta) d\zeta = \zeta + \frac{\alpha_* \zeta^2}{2},$$

and $\text{Heav}(\xi)$ denotes the Heaviside function.

Integration of the dimensionless growth rate from Equations (9) and (10) using variables (16) and (23) we arrive at

$$\frac{d\zeta}{dt} = \frac{v(t)}{1 + \alpha_* \zeta'}$$

and with the initial condition $\zeta = 0$ at $t = \nu$, we obtain

$$\alpha_* \zeta = \sqrt{1 + 2\alpha_* [\zeta(t) - \zeta(\nu)]} - 1. \tag{27}$$

Expression (27) determines the crystal radius $\zeta_m(t)$ in a dimensionless form (at $\nu = 0$) appearing as a function of time t .

Now we replace the variable ζ at any constant time t by the new variable ν as

$$\zeta(\nu) = \zeta(t) - \eta(\zeta).$$

Note that the limits $\zeta = \zeta_m(t)$ and $\zeta = 0$ of the integration over ζ correspond to the limits $\nu = t$ and $\nu = 0$ of the integration over ν , respectively. Hence, by substituting Equations (26) and (27) into expression (7), we arrive at

$$\frac{dv}{dt} = -B_1 v \int_0^t h(\nu, t) \exp[pg(\nu)] d\nu, \tag{28}$$

where

$$h(\nu, t) = \frac{\left\{ \sqrt{1 + 2\alpha_* [\zeta(t) - \zeta(\nu)]} - 1 \right\}^2}{\alpha_*^2 \sqrt{1 + 2\alpha_* [\zeta(t) - \zeta(\nu)]}}, \tag{29}$$

and $g(\nu) = g(\nu(\nu))$ is defined by Equations (21), (22), (24) or (25).

The integro-differential Equation (28) can be simplified if the dimensionless Gibbs number p is higher than unity and the nucleation is sufficiently intense. In this case, the Laplace-type integral (28) can be calculated using the saddle-point method.

Equations (21), (22), (24) and (25) introduce $\frac{dg}{d\nu} < 0$ for all kinetic mechanisms. This represents that the function $g(\nu)$ reaches the maximum at the boundary $\nu = 0$. Using the Equation (28) and calculating the derivatives of the function ν over ν , we arrive at first three derivatives that are equal to zero at $\nu = 0$, and $g^{(n)}|_{\nu=0} \neq 0$ at $n \geq 4$.

The first four derivatives are given in Table 1, where

$$\chi = \left(\frac{6}{B_1} \right)^{1/4}, \quad \kappa = \frac{1}{(1 + \nu_p) \ln^3(1 + \nu_p^{-1})}.$$

Thus, the saddle point method for an integral of Laplace type (28) gives the solution to the problem as follows [50]

$$\int_0^t h(\nu, t) \exp[pg(\nu)] d\nu \approx \sum_{k=0}^{\infty} p^{-(k+1)/4} a_k(\zeta(t)), \tag{30}$$

$$a_k(\zeta(t)) = (-1)^{k+1} \frac{4^k}{k!} \Gamma\left(\frac{k+1}{4}\right) H^k(0) \frac{d^k}{d\nu^k} [h(\nu, t) H(\nu)]_{\nu=0}, \tag{31}$$

where Γ represents the Euler gamma function, and

$$H(\nu) = \frac{[g(\nu)]^{3/4}}{g'(\nu)}.$$

Table 1. Functions and parameters of the analytic solution for various kinetics. Here $z = z(\zeta(t)) = 1 + 2\alpha_*\zeta(t)$, and ϕ_0, ϕ_1, ϕ_2 and ϕ_3 are given below.

Values	Supercooled Melts		Supersaturated Solutions	
	WVfZ Kinetics $I = I_* \exp\left[\frac{-p}{(\Delta T/\Delta T_0)^2}\right]$	Meirs Kinetics $I = I_*(\Delta T)^p$	WVfZ Kinetics $I = I_* \exp\left[\frac{-p}{\ln^2(C_i/C_p)}\right]$	Meirs Kinetics $I = I_*(\Delta C)^p$
$g^{(IV)} _{v=0}$	(6) and (16) (21)	(16) (22)	(7) and (23) (24)	(23) (25)
$g^{(V)} _{v=0}$	$-4B_1$	$-2B_1$	$-4\kappa B_1$	$-2B_1$
$g^{(VI)} _{v=0}$	$24B_1\alpha_*$	$12B_1\alpha_*$	$24\kappa B_1\alpha_*$	$12B_1\alpha_*$
$g^{(VII)} _{v=0}$	$-180B_1\alpha_*^2$	$-90B_1\alpha_*^2$	$-180\kappa B_1\alpha_*^2$	$-90B_1\alpha_*^2$
$H _{v=0}$	$1680B_1\alpha_*^3$	$840B_1\alpha_*^3$	$1680\kappa B_1\alpha_*^3$	$840B_1\alpha_*^3$
$H' _{v=0}$	$-\chi/4$	$-2^{1/4}\chi/4$	$-\kappa^{-1/4}\chi/4$	$-2^{1/4}\chi/4$
$H'' _{v=0}$	$-3\alpha_*\chi/20$	$-3\alpha_*2^{1/4}\chi/20$	$-3\kappa^{-1/4}\alpha_*\chi/20$	$-3\alpha_*2^{1/4}\chi/20$
$H''' _{v=0}$	$9\alpha_*^2\chi/50$	$9\alpha_*^22^{1/4}\chi/50$	$9\kappa^{-1/4}\alpha_*^2\chi/50$	$9\alpha_*^22^{1/4}\chi/50$
$H'''' _{v=0}$	$-57\alpha_*^3\chi/100$	$-57\alpha_*^32^{1/4}\chi/100$	$-57\kappa^{-1/4}\alpha_*^3\chi/100$	$-57\alpha_*^32^{1/4}\chi/100$
$v_0(z)$	$1 - \phi_0(z)$	$1 - 2^{1/4}\phi_0(z)$	$1 - \kappa^{-1/4}\phi_0(z)$	$1 - 2^{1/4}\phi_0(z)$
$v_1(z)$	$v_0(z) + \phi_1(z)$	$v_0(z) + \sqrt{2}\phi_1(z)$	$v_0(z) + \kappa^{-1/2}\phi_1(z)$	$v_0(z) + \sqrt{2}\phi_1(z)$
$v_2(z)$	$v_1(z) + \phi_2(z)$	$v_1(z) + 2^{3/4}\phi_2(z)$	$v_1(z) + \kappa^{-3/4}\phi_2(z)$	$v_1(z) + 2^{3/4}\phi_2(z)$
$v_3(z)$	$v_2(z) + \phi_3(z)$	$v_2(z) + 2\phi_3(z)$	$v_2(z) + \kappa^{-1}\phi_3(z)$	$v_2(z) + 2\phi_3(z)$

The first four coefficients in expression (31) have the form ($z = z(\zeta(t))$)

$$a_0(z) = -\Gamma\left(\frac{1}{4}\right)h(0,t)H(0), \quad a_1(z) = 4\Gamma\left(\frac{1}{2}\right)H(0)\left[H(0)\left(\frac{\partial h}{\partial v}\right)_{v=0} + h(0,t)H'(0)\right],$$

$$a_2(z) = -8\Gamma\left(\frac{3}{4}\right)H^2(0)\left[2H'(0)\left(\frac{\partial h}{\partial v}\right)_{v=0} + H(0)\left(\frac{\partial^2 h}{\partial v^2}\right)_{v=0} + h(0,t)H''(0)\right],$$

$$a_3(z) = \frac{32}{3}H^3(0)\left[3H''(0)\left(\frac{\partial h}{\partial v}\right)_{v=0} + h(0,t)H'''(0) + 3H'(0)\left(\frac{\partial^2 h}{\partial v^2}\right)_{v=0} + H(0)\left(\frac{\partial^3 h}{\partial v^3}\right)_{v=0}\right],$$

where H and its derivatives at the point $v = 0$ are given in Table 1, and

$$h(0,t) = \frac{(\sqrt{z}-1)^2}{\alpha_*^2\sqrt{z}}, \quad \left(\frac{\partial h}{\partial v}\right)_{v=0} = \frac{(\sqrt{z}-1)^2}{\alpha_*z^{3/2}} - 2\frac{\sqrt{z}-1}{\alpha_*z},$$

$$\left(\frac{\partial^2 h}{\partial v^2}\right)_{v=0} = \frac{3}{z^{5/2}} - \frac{1}{z^{3/2}}, \quad \left(\frac{\partial^3 h}{\partial v^3}\right)_{v=0} = \frac{15\alpha_*}{z^{7/2}} - \frac{3\alpha_*}{z^{5/2}}.$$

The functions $\phi_0(z), \phi_1(z), \phi_2(z)$, and $\phi_3(z)$ in Table 1, have the form

$$\phi_0 = \Gamma\left(\frac{1}{4}\right)\frac{B_1\chi(\sqrt{z}-1)^3}{12\alpha_*^3p^{1/4}}, \quad \phi_1 = \frac{\sqrt{6\pi B_1}(\sqrt{z}-1)^2(\sqrt{z}-z+5)}{20\alpha_*^2\sqrt{pz}},$$

$$\phi_2 = \Gamma\left(\frac{3}{4}\right)\frac{B_1\chi^3}{200\alpha_*p^{3/4}z^{3/2}}\left(25 + 5z - 66z^{3/2} + 48z^2 - 18z^{5/2} + 6z^3\right),$$

$$\phi_3 = \frac{75 + 20z - 99z^2 + 77z^{5/2} - 111z^3 + 57z^{7/2} - 19z^4}{100pz^{5/2}}.$$

Note that

$$z = z(\zeta(t)) = 1 + 2\alpha_*\zeta(t), \quad \zeta(t) = \int_0^t v(t)dt.$$

Substituting now

$$\frac{dv}{dt} = \frac{dv}{d\zeta} \frac{d\zeta}{dt} = v \frac{dv}{d\zeta}$$

to the left side of Equation (28) and taking expression (30) into account, we obtain the differential equation for dimensionless metastability degree

$$\frac{dv}{d\zeta} = -B_1 \sum_{k=0}^{\infty} p^{-(k+1)/4} a_k(\zeta).$$

By integrating it, we obtain the solution for v as

$$v(\zeta) = -B_1 p^{-1/4} \int_0^{\zeta} \sum_{k=0}^{\infty} p^{-k/4} a_k(\zeta) d\zeta + 1. \quad (32)$$

Further, we find an expression for $t(\zeta)$ to determine v as a function of time t . Substituting $v(\zeta)$ from (32) into the relation $v = d\zeta/dt$, we obtain

$$t(\zeta) = \int_0^{\zeta} \frac{d\zeta}{v(\zeta)}. \quad (33)$$

The Equations (32) and (33) determine the dimensionless metastability degree v as a function of time t in parametric form. Figure 1 shows this function for the two mechanisms of kinetic crystal growth from supercooled melt, where $v = v_0$ is the main contribution to the sum in expression (32) and $v = v_i$ ($i = 1, 2, 3$) represents the i -approximation of the complete solution for v

$$v = v_i = -B_1 p^{-1/4} \int_0^{\zeta} \sum_{k=0}^i p^{-k/4} a_k(\zeta) d\zeta + 1.$$

Figure 1 illustrates dimensionless supercooling v to the dimensionless time t . If the melt was initially supercooled (see Figure 1a,b), the rate of supercooling removal is high (this can be explained mathematically by the inflection point in the Figure 1b for small t). Otherwise, v_2 and v_3 in Figure 1b,c show that the initially fast rate of metastability removal decreases with time as nucleation slows and coarsening of existing crystallites continues.

The given solutions allow us to determine an equation for the density function of crystal size distribution. Considering the maximum size of crystals appearing at the zero moment of time

$$\zeta_m(\zeta(t)) = \frac{\sqrt{1 + 2\alpha_* \zeta(t)} - 1}{\alpha_*}, \quad (34)$$

we arrive at

$$\Phi(\zeta(t), \zeta) = (1 + \alpha_* \zeta) E_1^{-1}(t, \zeta) \exp \left[-\frac{p(1 - E_1^2)}{E_1^2} \right], \quad (35)$$

where

$$E_1(\zeta(t), \zeta) = 1 - B_1 \int_0^{\zeta(t) - \zeta - \alpha_* \zeta^2 / 2} \sum_{k=0}^{\infty} p^{-(k+1)/4} a_k(\zeta) d\zeta.$$

Here ζ is limited by ζ_m , $\zeta(t)$ is defined by (33) as an inverse function.

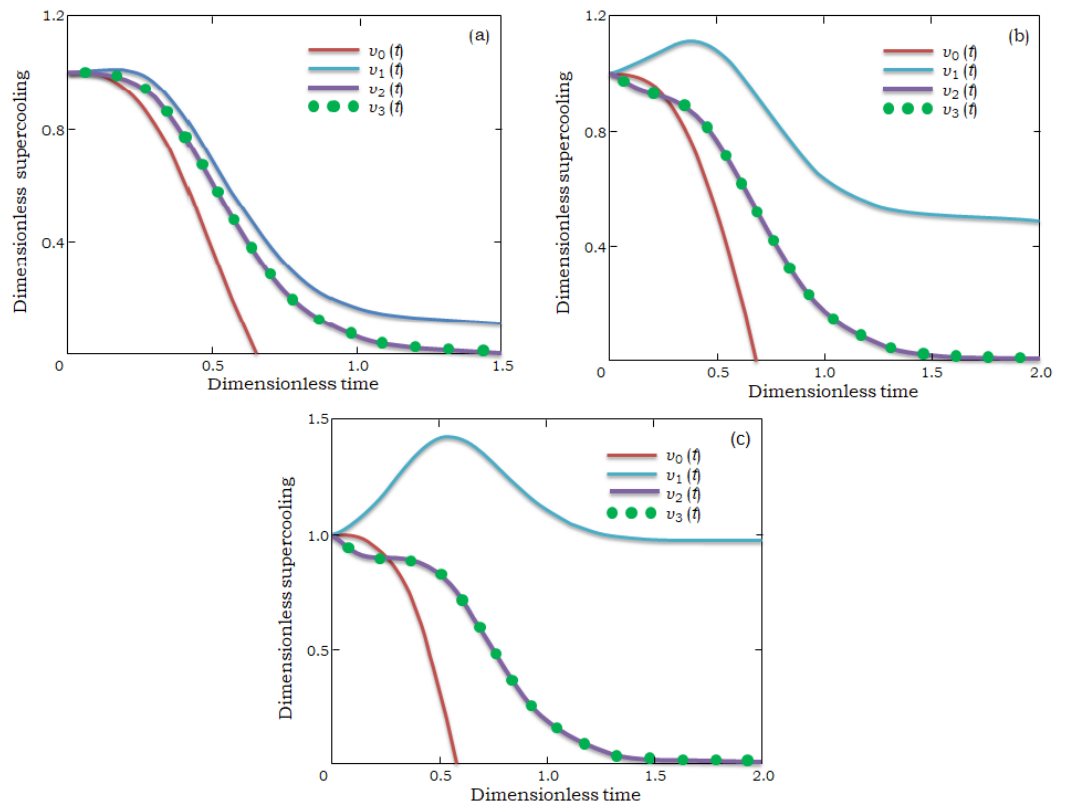


Figure 1. Dimensionless supercooling $v = \frac{\Delta T}{\Delta T_0}$ as a function of dimensionless time $t = \frac{\tau}{\tau_0}$: (a) WWFZ kinetics at $\Delta T_0 = 373$ K, $p = 66.9$; (b) WWFZ kinetics at $\Delta T_0 = 573$ K, $p = 7.4$; (c) Meirs kinetics at $\Delta T_0 = 573$ K, $p = 4$. The physical parameters are typical for supercooled melts [52–54]: $\gamma_i = 0.3$ J m $^{-2}$, $L_V = 7 \times 10^9$ J m $^{-3}$, $T_p = 1273$ K, $\rho_s = 7.8 \times 10^3$ kg m $^{-3}$, $\rho_m = \rho_l = 7 \times 10^3$ kg m $^{-3}$, $\beta_* = 0.5 \times 10^{-7}$ m/s $^{-1}$ K $^{-1}$, $\lambda_l = 63$ J m $^{-1}$ K $^{-1}$ s $^{-1}$, $I_0 = 10^{11}$ m $^{-3}$ s $^{-1}$, $C_m = 840$ Jkg $^{-1}$ K $^{-1}$.

Figure 2 represents the evolution of the dimensionless density of the distribution function Φ . It can be seen that weak inflection points appear as time increases. This means that the high nucleation rate is typical for the initial stage of the process when supercooling/supersaturation is close to the value $v = 1$. The nucleation process is followed by coarsening of the crystallites, which reduces the metastability degree of the system, slows down the intensity of nucleation, and leads to inflection points on the density graphs of the distribution function. It is important to note that such behavior was previously observed in experiments (see, for example, [55–58]).

The total number of crystals in the metastable system is an important parameter for the intermediate stage of phase transitions

$$N(\xi(t)) = \frac{1}{l_0^3} \int_0^{\zeta_m(\xi(t))} \Phi(\xi(t), \zeta) d\zeta, \quad (36)$$

where $\zeta_m(\xi)$ and $\xi(t)$ are defined by expressions (33) and (34). The other important parameter of evolving particulate ensembles is the average size of crystals

$$\bar{L}(\xi(t)) = l_0 \int_0^{\zeta_m(\xi(t))} \zeta \Phi d\zeta \left(\int_0^{\zeta_m(\xi(t))} \Phi d\zeta \right)^{-1}. \quad (37)$$

Equations (36) and (37) are complete solutions written in parametric form.

The dimensionless number of crystals $n_i(t)$ and average crystal size $u_i(t)$, corresponding to the i -approximation of the solution (35), are shown in Figure 3 (functions u_i and n_i are defined below). It is easy to see that approximations n_2 and u_2 correspond to the third-order solutions n_3 and u_3 . It is important to note the stability of the characteristics with increasing time at the intermediate stage of the phase transformation process, while the main contributions n_0 and u_0 previously found in [35], give only a rough approximation to the solution behavior.

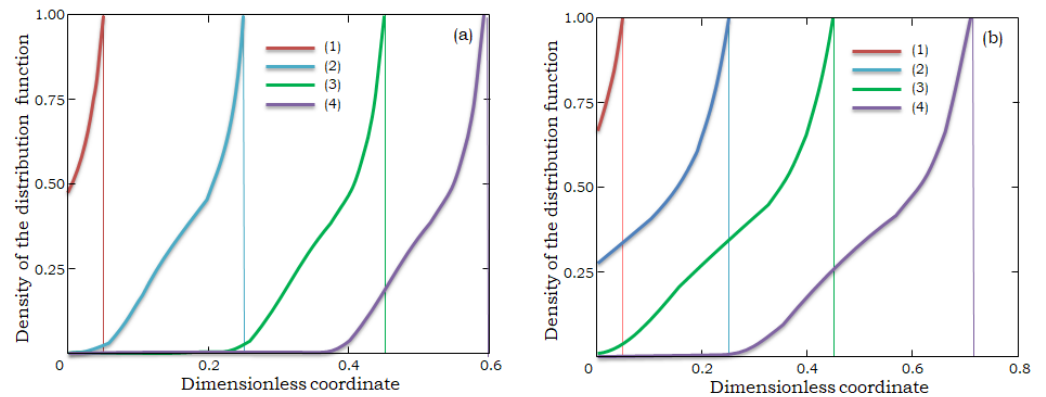


Figure 2. The dimensionless distribution function $\Phi(t, \zeta)$ as a function of $\zeta = \frac{r}{l_0}$ at different times $t = \frac{\tau}{t_0}$ for supercooled melts with WVFZ kinetics: (a) $p = 669, \Delta T_0 = 373$ K, (1) $t = 0.05, \zeta = 0.05$, (2) $t = 0.254, \zeta = 0.25$, (3) $t = 0.503, \zeta = 0.45$, and (4) $t = 1.513, \zeta = 0.591$; (b) $p = 7.4, \Delta T_0 = 573$ K, (1) $t = 0.051, \zeta = 0.05$, (2) $t = 0.263, \zeta = 0.25$, (3) $t = 0.496, \zeta = 0.45$, and (4) $t = 1.95, \zeta = 0.71$. The maximal size ζ_m of crystals is shown by vertical lines at different moments of time. The curves denoted by simbole (4) corresponding to the moment when supercooling is removed ($v = 0$).

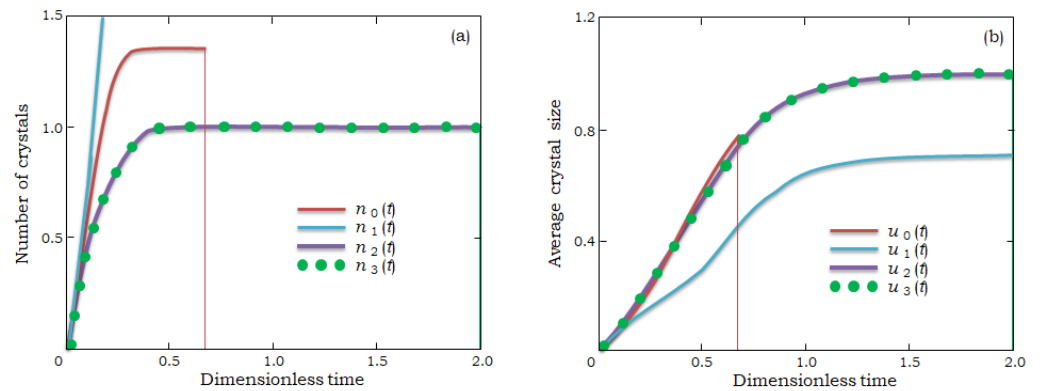


Figure 3. The dimensionless number of crystals $n_i = \frac{N_i(\zeta)}{N_3(\zeta_*)}$ (a) and average crystal size $u_i = \frac{\bar{L}_i(\zeta)}{\bar{L}_3(\zeta_*)}$ (b) as a function of dimensionless time $t = \frac{\tau}{t_0}$ for supercooled melts with WVFZ kinetics, $p = 7.4, \Delta T_0 = 573$ K. The vertical lines show the time of the process when supercooling is totally removed.

The number N_i of crystals and the average crystal size \bar{L}_i , corresponding to the i -approximation of the solution can be written as

$$N_i(\zeta(t)) = \frac{1}{l_0^3} \int_0^{\zeta_m(\zeta(t))} \Phi_i(\zeta(t), \zeta) d\zeta, \bar{L}_i(\zeta(t)) = l_0 \int_0^{\zeta_m(\zeta(t))} \zeta \Phi_i d\zeta \left(\int_0^{\zeta_m(\zeta(t))} \Phi_i d\zeta \right)^{-1},$$

where

$$\Phi_i(\zeta(t), \zeta) = (1 + \alpha_* \zeta) E_{1i}^{-1}(t, \zeta) \exp \left[-\frac{p(1 - E_{1i}^2)}{E_{1i}^2} \right],$$

$$E_{1i}(\xi(t), \zeta) = 1 - B_1 \int_0^{\xi(t) - \zeta - \alpha_* \zeta^2 / 2} \sum_{k=0}^i p^{-(k+1)/4} a_k(\xi) d\xi.$$

The relative number of particles n_i and the average crystal radius u_i , shown in Figure 3, can be written in the form

$$n_i(\xi(t)) = \frac{N_i(\xi(t))}{N_3(\xi_*)}, \quad u_i(\xi(t)) = \frac{L_i(\xi(t))}{L_3(\xi_*)},$$

where, the parameter ξ_* corresponds to the time t_* when supercooling/supersaturation of the system is completely removed. This dependence is defined by Equation (33), where $t_* = t(\xi_*)$.

4. The Model with Fluctuations in Crystal Growth Rates

Experiments demonstrate that the crystal growth rate has random fluctuations [59–62] occurring a random crystal radius $r(\tau)$. Thus, the kinetic equation for the density ϕ can be written as

$$\frac{\partial \phi}{\partial \tau} + \frac{\partial}{\partial r} \left(\frac{dr}{d\tau} \phi \right) = \frac{\partial}{\partial r} \left(D \frac{\partial \phi}{\partial r} \right), \quad \tau > 0, \quad r > r_*, \quad (38)$$

where D is a function determining fluctuation rate. Then, equating the crystal flux of minimum size r_* to the nucleation frequency I , the boundary conditions are found as

$$\frac{dr}{d\tau} \phi - D \frac{\partial \phi}{\partial r} = I(\Delta T), \quad r = r_*, \quad \tau > 0, \quad (39)$$

$$\phi = 0, \quad r \rightarrow \infty, \quad (40)$$

where

$$\frac{dr}{d\tau} = \beta_* \Delta T, \quad (41)$$

$$D = d_1 \frac{dr}{d\tau} = \beta_* d_1 \Delta T. \quad (42)$$

Parameter d_1 is the proportionality constant. Note that this theoretical assumption is also confirmed experimentally [63]. Thus, the equations and conditions (12), (13), (38)–(42) represent the complete statement of the problem.

Let us now rewrite this problem statement in dimensionless variables (16) ($\Phi = \Phi(t, \zeta)$, $r_* \rightarrow 0$, $v = v(t)$) as

$$\frac{\partial \Phi}{\partial t} + v \frac{\partial \Phi}{\partial \zeta} = u_0 v \frac{\partial^2 \Phi}{\partial \zeta^2}, \quad t > 0, \quad \zeta > 0, \quad (43)$$

$$\Phi = 0, \quad \zeta \rightarrow \infty, \quad (44)$$

$$v = 1 - B \int_0^\infty \zeta^3 \Phi(t, \zeta) d\zeta, \quad t > 0, \quad (45)$$

$$J(v) \equiv \frac{1}{v} \exp[p\varphi(v)] = \Phi - u_0 \frac{\partial \Phi}{\partial \zeta}, \quad \zeta = 0. \quad (46)$$

Here $B = B_1/3$, $u_0 = d_1/l_0$, Equation (45) is time-integrated with (38). Initial conditions (19) in the case of WVFZ kinetics can be written as $\varphi(v) = 1 - v^{-2}$ and in the case of Meirs kinetic as $\varphi(v) = \ln(v)$.

Entering the modified time

$$\xi(t) = \int_0^t v(t_1) dt_1,$$

we rewrite Equation (43) in the following form ($v = v(\xi), \Phi = \Phi(\xi, \zeta)$)

$$\frac{\partial \Phi}{\partial \xi} + \frac{\partial \Phi}{\partial \zeta} = u_0 \frac{\partial^2 \Phi}{\partial \zeta^2}, \quad \xi > 0, \quad \zeta > 0. \tag{47}$$

The equation may be solved using the Laplace integral method (the initial condition gives $\xi = 0$ and $\Phi = 0$).

Considering the boundary conditions (44) and (46), we write the final solution of Equation (47) as

$$\begin{aligned} \Phi(\xi, \zeta) = & \exp\left(\frac{\zeta}{2u_0}\right) \int_0^\xi \frac{J[v(\xi - \eta)]}{\sqrt{u_0}} \exp\left(-\frac{\eta}{4u_0}\right) \left[\frac{1}{\sqrt{\pi\eta}} \exp\left(-\frac{\zeta^2}{4u_0\eta}\right) \right. \\ & \left. - \frac{1}{2\sqrt{u_0}} \exp\left(\frac{\zeta}{2u_0} + \frac{\eta}{4u_0}\right) \operatorname{erfc}\left(\frac{\zeta}{2\sqrt{u_0\eta}} + \frac{\sqrt{\eta}}{2\sqrt{u_0}}\right) \right] d\eta. \end{aligned} \tag{48}$$

Substituting the Equation (48) into (45) and evaluating the integral over ζ , we obtain

$$v(\xi) = 1 - B \int_0^\xi J[v(\xi - \eta)]h(\eta)d\eta, \tag{49}$$

where

$$\begin{aligned} h(\eta) = & \frac{2}{\sqrt{\pi}} \left[\exp\left(-\frac{\eta}{4u_0}\right) \left(\frac{1}{2}u_0^{1/2}\eta^{5/2} + \frac{7}{2}u_0^{3/2}\eta^{3/2} - 3u_0^{5/2}\eta^{1/2} \right) \right. \\ & \left. + \sqrt{\pi} \left(\frac{9}{2}u_0\eta^2 + 3u_0^3 + \frac{\eta^3}{2} \right) \right] - \operatorname{erfc}\left(\frac{\sqrt{\eta}}{2\sqrt{u_0}}\right) \left[6u_0^3 + \frac{9}{2}u_0\eta^2 + \frac{\eta^3}{2} \right], \\ J[v(\xi - \eta)] = & \frac{1}{v(\xi - \eta)} \exp\{p\varphi[v(\xi - \eta)]\}. \end{aligned}$$

Next, we replace the variable by the inverse function $\eta = \eta(v)$ to solve the Equation (49) and arrive at

$$v = 1 - B \int_1^v J(v_1)h[\eta(v_1)] \frac{d\eta}{dv_1} dv_1. \tag{50}$$

Differentiating the Equation (50) over the variable v gives an equation with separate variables, the integration of which determines the implicit expression for $v(\xi)$ as

$$\int_1^v \frac{dv_1}{J(v_1)} = \int_1^v v_1 \exp[-p\varphi(v_1)]dv_1 = -B \int_0^\xi h(\eta)d\eta \equiv H(\xi). \tag{51}$$

Substituting the expressions for φ , we find $v(\xi)$ for WVFZ kinetics in a form

$$v^2 \exp\left[-p\left(1 - \frac{1}{v^2}\right)\right] - 1 - p \exp(-p)E_p(v) = 2H(\xi), \tag{52}$$

and for Meirs kinetics

$$v(\xi) = [(2 - p)H(\xi) + 1]^{1/(2-p)}, \quad p \neq 2; \quad v(\xi) = \exp[H(\xi)], \quad p = 2. \tag{53}$$

Here $E_p(\zeta)$ denotes the integral function

$$E_p(v) = \int_p^{p/v^2} \frac{\exp(v)dv}{v}.$$

The analytical solutions (51)–(53) satisfy the integral Equation (49).

Given the density of the distribution function (48), find the number N of crystals as a function of the parameter ξ

$$N = \int_0^\infty \phi(\tau, r) dr = \frac{1}{l_0^3} \int_0^\infty \Phi(\xi, \zeta) d\zeta = \frac{1}{l_0^3} \int_0^\xi J[v(\xi - \eta)] d\eta. \tag{54}$$

Now rewriting $\zeta(t)$, we obtain the solution with parameter ξ as

$$t(\xi) = \int_0^\xi \frac{d\zeta_1}{v(\zeta_1)}. \tag{55}$$

Equations (48), (51)–(55) are exact analytical solutions of the integro-differential model describing nucleation and growth of crystals at the intermediate stage of phase transitions. The solution is expressed in a general form that is valid for various kinetic mechanisms.

Figures 4 and 5 show an exact analytical solutions according to expressions (48), (53), and (55) for Meirs nucleation kinetics. It can be seen that the removal of supercooling slows down with time when the nucleation process is not intense enough (when ξ is greater than or near unity in Figure 4), while the density of the distribution function becomes larger with increasing time (when ξ increases in Figure 5).

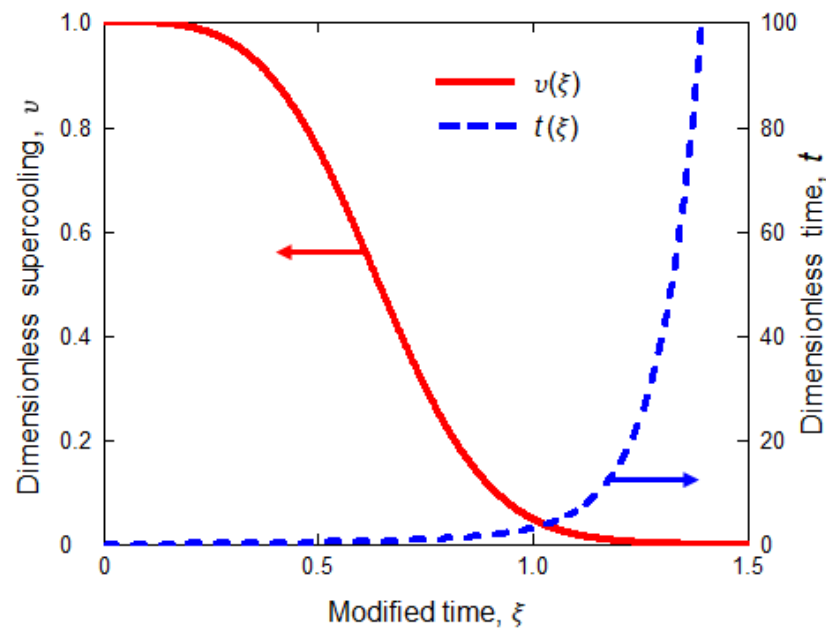


Figure 4. The dimensionless supercooling $v = \frac{\Delta T}{\Delta T_0}$ and time $t = \frac{\tau}{\xi_0}$ depending on the modified time ξ . The physical parameters are typical for metallic alloys: $u_0 = 10^{-2}$, $B = 14.92$, $\Delta T_0 = 300$ °C, $p = 2.2$.

Figure 6 demonstrates the transition from a bell-shaped distribution to a distribution with a break point as the parameter u_0 decreases. When u_0 is small enough, the distribution function has the behavior described, for example, in [64], where the early stages of the Ostwald ripening process were observed. It shows that the diffusion term in Equation (38) is important in the initial stages of the intermediate phase transition. Figure 7 compares the theory with experimental data on crystallization kinetics of lysozyme and canavalin. The metastability reduction is in good agreement with experimental data for a broad range of time changes, as can easily be seen. Significantly, the analytical method defining the intermediate stage of phase transitions can be applied to determine the initial crystal

distribution at the final stage of phase transformation and the Ostwald ripening stage (when the supercooling of the system tends to zero).

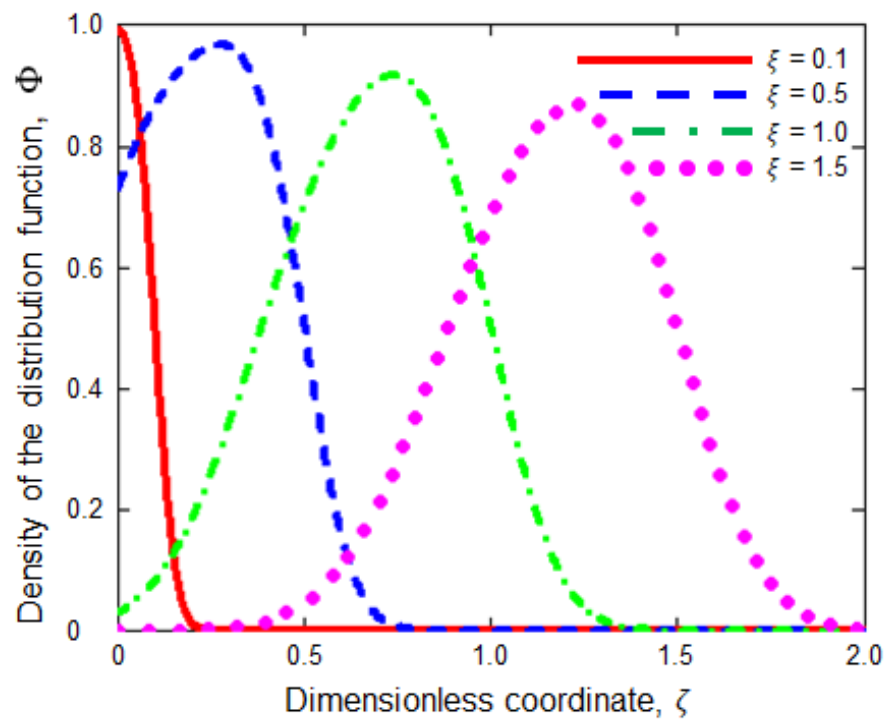


Figure 5. The dimensionless density of the distribution function Φ as a function of the crystal radius at different time moments.

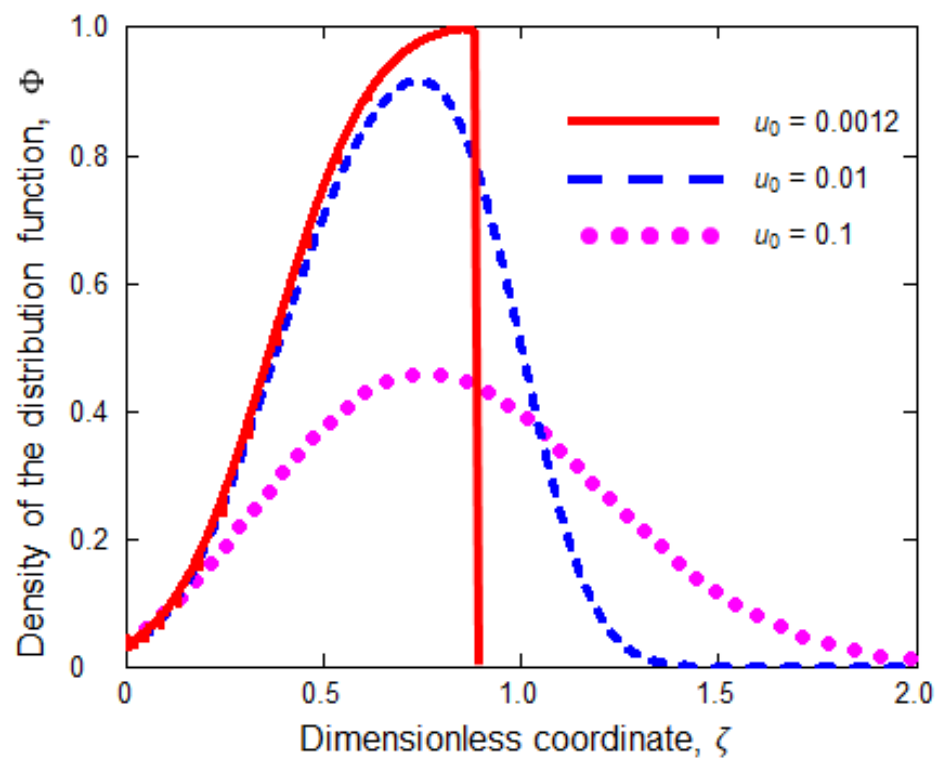


Figure 6. The dimensionless density of the distribution function Φ as a function of the crystal radius at different values of the parameter u_0 ($\xi = 1$).

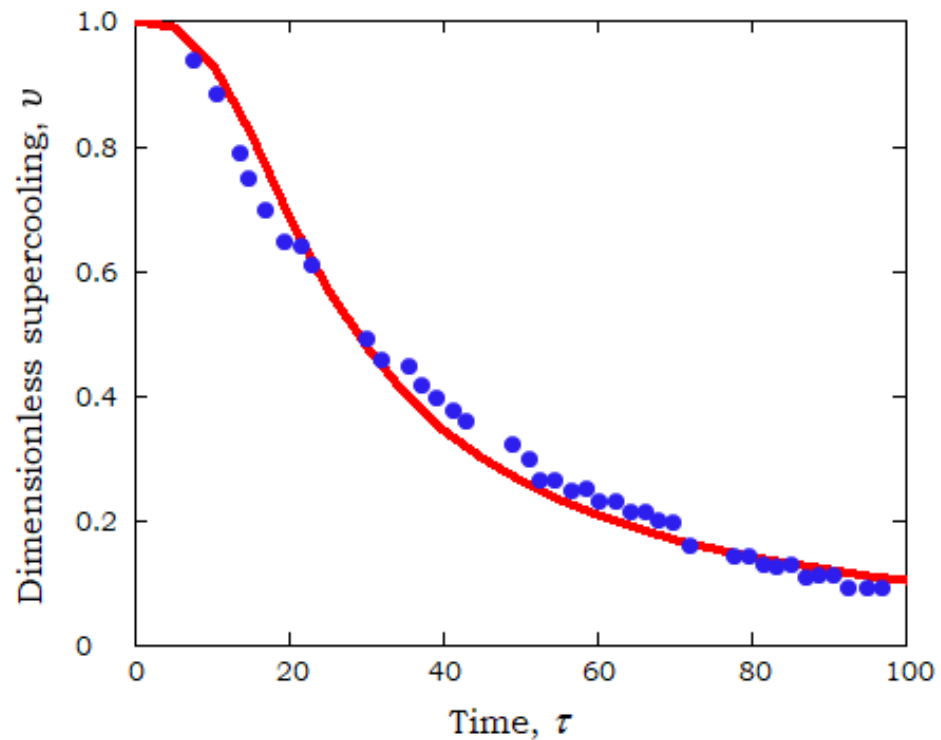


Figure 7. Comparison of theory (solid line) with experiment (dots) [65]. Calculated parameters in Equation (53): $u_0 = 10^{-1}$, $p = 4.5$.

5. Conclusions

This paper deals with the intermediate stage of a phase transformation in one-component metastable systems (melts or solutions). The main results are as follows:

- (i) A complete analytic solution of the integro-differential model that describes the intermediate phase transition in one-component melts and solutions without taking into account fluctuations in the crystal growth rate has been found. Within the framework of this model, an exact analytical solution of the kinetic equation is obtained, and the density of the crystal size distribution function is found. An integro-differential equation for the metastability degree has been derived. A complete analytical solution to this equation is constructed based on the saddle-point method for calculating the Laplace-type integral.
- (ii) Our studies show that the found second approximation of the asymptotic solution is sufficient for quantitative analysis of the solution to the problem. In other words, our study demonstrates the sign-variable convergence of solutions to the second approximation, which indicates the fundamental importance of taking into account the first and second corrections in the asymptotic solution of the problem. The convergence of the found solution is ensured by a large value of the dimensionless Gibbs number p and/or by the smallness of the parameter α_* , which is typical for a wide class of real systems. An explicit form of the first four coefficients of the found asymptotic solutions for the Weber-Volmer-Frenkel-Zel'dovich and Meiers nucleation kinetics is derived.
- (iii) Within the framework of the obtained solution, it is shown that the metastability degree and density of the distribution function have inflection points (observed experimentally) responsible for different stages of the phase transition process. At the initial times, when supercooling/supersaturation is large, the appearance of nuclei is the dominant process; then this process is followed by the growth of crystallites, which

- becomes dominant at the final stages of the intermediate phase transition when the metastability of the system is sufficiently small and nucleation proceeds unintensively.
- (iv) An exact analytical solution has been found for an integro-differential model describing the intermediate stage of the phase transition in one-component melts and solutions taking fluctuations in the crystal growth rate into account. Namely, the density of the crystal size distribution function has been determined and an implicit expression for metastability degree of the system in the case of different nucleation kinetics has been driven. The parametric solution to the problem constructed in this work is detailed for the frequently encountered Weber-Volmer-Frenkel-Zel'dovich and Meirs nucleation kinetics.
 - (v) It is shown that the exact analytical solution to the integro-differential model with allowance for the “diffusion” term in the Fokker-Planck equation passes into a complete solution of the “non-diffusion” model (when the “diffusion” term in the kinetic equation is small enough). The analytical solutions, describing the evolution of the phase transformation at the intermediate stage, can be used as initial conditions at the final stage of the phase transition (e.g., at the stage of Ostwald ripening or coagulation of crystals).

In general, the paper shows methods for solving the kinetic and balance equations for the intermediate stage of phase transformation with and without considering fluctuations in crystal growth rates (respectively in the case of the kinetic equation of second and first orders). The solutions found can be used as initial conditions for the final phase of the phase transformation, which is described by different models with consideration of Ostwald ripening of the particles, their possible coagulation, and fragmentation [66–70]. The theory developed in this paper may be generalized to the case of a simultaneous phase transformation in the volume of the metastable phase and in a given spatial direction (directional phase transition), which is caused by the presence of temperature gradients. This situation occurs when crystals grow in the moving region of the phase transformation—the two-phase layer. A theory combining volumetric and directional phase transformation can be developed in the spirit of Refs. [71–80].

Author Contributions: Conceptualization, L.V.T., E.V.M. and D.V.A.; methodology, D.V.A.; software, L.V.T., E.V.M. and S.I.O.; validation, E.V.M. and A.P.M.; formal analysis, A.P.M. and E.V.M.; investigation, E.V.M.; resources, L.V.T.; writing—original draft preparation, L.V.T., Y.Y. and D.V.A.; writing—review and editing, Y.Y. and D.V.A.; visualization, L.V.T.; supervision, E.V.M. and D.V.A.; project administration, L.V.T.; funding acquisition, L.V.T., E.V.M. and S.I.O. All authors have read and agreed to the published version of the manuscript.

Funding: Authors gratefully acknowledge financial support from the Russian Science Foundation (project no. 21-79-10012).

Institutional Review Board Statement: Not applicable.

Informed Consent Statement: Not applicable.

Data Availability Statement: All data generated or analysed during this study are included in this published article.

Conflicts of Interest: The authors declare no conflict of interest.

References

1. Madras, G.M.; McCoy, B.J. Transition from nucleation and growth to Ostwald ripening. *Chem. Eng. Sci.* **2002**, *57*, 3809–3818. [[CrossRef](#)]
2. Zhang, T.H.; Liu, X.Y. Nucleation: What happens at the initial stage. *Angew. Chem. Int. Ed.* **2009**, *48*, 1308–1312. [[CrossRef](#)] [[PubMed](#)]
3. Uwaha, M.; Koyama, K. Transition from nucleation to ripening in the classical nucleation model. *J. Cryst. Growth* **2010**, *312*, 1046–1054. [[CrossRef](#)]
4. Makoveeva, E.V.; Alexandrov, D.V. On the theory of phase transformation process in a binary supercooled melt. *Eur. Phys. J. Spec. Top.* **2020**, *229*, 375–382. [[CrossRef](#)]

5. Alexandrov, D.V.; Alexandrova, I.V. On the theory of the unsteady-state growth of spherical crystals in metastable liquids. *Phil. Trans. R. Soc. A* **2019**, *377*, 20180209. [[CrossRef](#)]
6. Chernov, A.A. *Modern Crystallography III*; Springer: Berlin/Heidelberg, Germany, 1984.
7. Alexandrova, I.V.; Alexandrov, D.V. Dynamics of particulate assemblages in metastable liquids: A test of theory with nucleation and growth kinetics. *Phil. Trans. R. Soc. A* **2020**, *378*, 20190245. [[CrossRef](#)]
8. Chalmers, B. *Physical Metallurgy*; Wiley: New York, NY, USA, 1959.
9. Todes, O.M.; Seballo, V.A.; Gol'tsiker, L.D. *Bath Crystallization from Solutions*; Khimia: Leningrad, Russia, 1984.
10. Poon, J.M.-H.; Immanuel, C.D.; Doyle, F.J., III; Litsers, J.D. A three-dimensional population balance model of granulation with a mechanistic representation of the nucleation and aggregation phenomena. *Chem. Eng. Sci.* **2008**, *63*, 1315–1329. [[CrossRef](#)]
11. Poon, J.M.-H.; Ramachandran, R.; Sanders, C.F.W.; Glaser, T.; Immanuel, C.D.; Doyle, F.J., III; Litsers, J.D.; Stepanek, F.; Wang, F.Y.; Cameron, I.T. Experimental validation studies on a multi-scale and multi-dimensional population balance model of batch granulation. *Chem. Eng. Sci.* **2009**, *64*, 775–786. [[CrossRef](#)]
12. Alexandrov, D.V.; Dubovoi, G.Y.; Malygin, A.P.; Nizovtseva, I.G.; Toropova, L.V. Solidification of ternary systems with a nonlinear phase diagram. *Russ. Metall.* **2017**, *2017*, 127–135. [[CrossRef](#)]
13. Makoveeva, E.V.; Alexandrov, D.V.; Ivanov, A.A. Mathematical modeling of crystallization process from a supercooled binary melt. *Math. Meth. Appl. Sci.* **2021**, *44*, 12244–12251. [[CrossRef](#)]
14. Thompson, C.V.; Spaepen, F. Homogeneous crystal nucleation in binary metallic melts. *Acta Metall.* **1983**, *31*, 2021–2027. [[CrossRef](#)]
15. Kelton, K.F.; Greer, A.L. *Nucleation in Condensed Matter: Applications in Materials and Biology*; Elsevier: Amsterdam, The Netherlands, 2010.
16. Zettlemoyer, A.C. *Nucleation*; Dekker: New York, NY, USA, 1969.
17. Alexandrov, D.V.; Nizovtseva, I.G.; Alexandrova, I.V. On the theory of nucleation and nonstationary evolution of a polydisperse ensemble of crystals. *Int. J. Heat Mass Trans.* **2019**, *128*, 46–53. [[CrossRef](#)]
18. Alexandrov, D.V. Kinetics of particle coarsening with allowance for Ostwald ripening and coagulation. *J. Phys. Condens. Matter* **2016**, *28*, 035102. [[CrossRef](#)] [[PubMed](#)]
19. Volmer, M. *Kinetik der Phasenbildung*; Steinkopf: Dresden, Germany, 1939.
20. Frenkel, J. *Kinetic Theory of Liquids*; Dover: New York, NY, USA, 1955.
21. Velmurugan, J.; Noel, J.-M.; Nogala, W.; Mirkin, M.V. Nucleation and growth of metal on nanoelectrodes. *Chem. Sci.* **2012**, *3*, 3307–3314. [[CrossRef](#)]
22. Lifshitz, I.M.; Slyozov V.V. The kinetics of precipitation from supersaturated solid solutions. *J. Phys. Chem. Solids* **1961**, *19*, 35–50. [[CrossRef](#)]
23. Tokuyama, M.; Kawasaki, M.; Enomoto, V. Kinetic equations for Ostwald ripening. *Physics A* **1986**, *134*, 323–338. [[CrossRef](#)]
24. Akaiwa, N.; Meiron, D.I. Numerical simulation of two-dimensional late-stage coarsening for nucleation and growth. *Phys. Rev. E* **1995**, *51*, 5408–5421. [[CrossRef](#)]
25. Farjoun, Y.; Neu, J.C. Aggregation according to classical kinetics: from nucleation to coarsening. *Phys. Rev. E* **2011**, *83*, 051607. [[CrossRef](#)]
26. Alexandrova, I.V.; Alexandrov, D.V.; Makoveeva, E.V. Ostwald ripening in the presence of simultaneous occurrence of various mass transfer mechanisms: An extension of the Lifshitz-Slyozov theory. *Phil. Trans. R. Soc. A* **2021**, *379*, 20200308. [[CrossRef](#)]
27. Alexandrov, D.V. On the theory of Ostwald ripening: Formation of the universal distribution. *J. Phys. A Math. Theor.* **2015**, *48*, 035103. [[CrossRef](#)]
28. Alexandrov, D.V. Relaxation dynamics of the phase transformation process at its ripening stage. *J. Phys. A Math. Theor.* **2015**, *48*, 245101. [[CrossRef](#)]
29. Avrami, M. Granulation, phase change, and microstructure kinetics of phase change. III. *J. Chem. Phys.* **1991**, *9*, 177–184. [[CrossRef](#)]
30. Aastuen, D.J.W.; Clark, N.A.; Swindal, J.C.; Muzny, C.D. Determination of the colloidal crystal nucleation rate density. *Phase Trans.* **1990**, *21*, 139–155. [[CrossRef](#)]
31. Binder, K.; Stauffer, D. Statistical theory of nucleation, condensation and coagulation. *Adv. Phys.* **1976**, *25*, 343–396. [[CrossRef](#)]
32. Langer, J.S.; Schwartz, A.J. Kinetics of nucleation in near-critical fluids. *Phys. Rev. A* **1980**, *21*, 948–958. [[CrossRef](#)]
33. Shneidman, V.A. Transient nucleation with a monotonically changing barrier. *Phys. Rev. E* **2010**, *82*, 031603. [[CrossRef](#)]
34. Shneidman, V.A. Time-dependent distributions in self-quenching nucleation. *Phys. Rev. E* **2011**, *84*, 031602. [[CrossRef](#)]
35. Buyevich, Y.A.; Mansurov, V.V. Kinetics of the intermediate stage of phase transition in batch crystallization. *J. Cryst. Growth* **1990**, *104*, 861–867. [[CrossRef](#)]
36. Buyevich, Y.A.; Ivanov, A.O. Kinetics of phase separation in colloids II. Non-linear evolution of a metastable colloid. *Physics A* **1993**, *193*, 221–240. [[CrossRef](#)]
37. Ivanov, A.O.; Zubarev, A.Y. Non-linear evolution of a system of elongated droplike aggregates in a metastable magnetic fluid. *Physics A* **1998**, *251*, 348–367. [[CrossRef](#)]
38. Barlow, D.A. Theory of the intermediate stage of crystal growth with applications to protein crystallization. *J. Cryst. Growth* **2009**, *311*, 2480–2483. [[CrossRef](#)]
39. Barlow, D.A.; Baird, J.K.; Su, C.-H. Theory of the von Weimarn rules governing the average size of crystals precipitated from a supersaturated solution. *J. Cryst. Growth* **2004**, *264*, 417–423. [[CrossRef](#)]
40. Volmer, M.; Weber, A. Nucleation in übersättigten Strukturen. *Z. Phys. Chem.* **1926**, *119*, 277–301. [[CrossRef](#)]

41. Zel'dovich, J.B. On the theory of formation of new phases: Cavitation. *J. Exp. Theor. Phys.* **1942**, *12*, 525–538.
42. Lifshitz, E.M.; Pitaevskii, L.P. *Physical Kinetic*; Pergamon Press: Oxford, UK, 1981.
43. Landau, L.D.; Lifshitz, E.M. *Statistical Physics*; Pergamon Press: Oxford, UK, 1980.
44. Mullin, J.W. *Crystallization*; Butterworths: London, UK, 1972.
45. Gherras, N.; Fevotte, G. Comparison between approaches for the experimental determination of metastable zone width: A case study of the batch cooling crystallization of ammonium oxalate in water. *J. Cryst. Growth* **2012**, *342*, 88–98. [[CrossRef](#)]
46. Kidyarov, B.I. *Kinetics of Crystal Formation from the Liquid Phase*; Nauka Publishing House: Novosibirsk, Russia, 1979.
47. Alexandrov, D.V.; Alexandrova, I.V.; Ivanov, A.A.; Malygin, A.P.; Starodumov, I.O.; Toropova, L.V. On the Theory of the Nonstationary Spherical Crystal Growth in Supercooled Melts and Supersaturated Solutions. *Russ. Metall.* **2019**, *2019*, 787–794. [[CrossRef](#)]
48. Nyvlt, J.; Sohnel, O.; Matuchova, M.; Broul, M. *The Kinetics of Industrial Crystallization*; Elsevier: Amsterdam, The Netherlands, 1985.
49. Randolph, A.; Larson, M. *Theory of Particulate Processes*; Academic Press: New York, NY, USA, 1988.
50. Fedoruk, M.V. *Saddle-Point Method*; Nauka: Moscow, Russia, 1977.
51. Alexandrov, D.V. Nonlinear dynamics of polydisperse assemblages of particles evolving in metastable media. *Eur. Phys. J. Spec. Top.* **2020**, *229*, 383–404. [[CrossRef](#)]
52. Skripov, V.P. *Methastable Liquids*; Wiley: New York, NY, USA, 1974.
53. Porter, D.A.; Easterling, K.E. *Phase Transformations in Metals and Alloys*; Van Nostrand Reinhold: New York, NY, USA, 1981.
54. Hamza, M.A.; Berge, B.; Mikosch, W.; Ruhl, E. Homogeneous nucleation of supersaturated KCl-solutions from single levitated microdroplets. *Phys. Chem. Chem. Phys.* **2004**, *6*, 3484–3489. [[CrossRef](#)]
55. Janse, A.H. *Nucleation and Crystal Growth in Batch Crystallizers*; Delft University of Technology: Delft, The Netherlands, 1977.
56. Pot, A. *Industrial Sucrose Crystallization*; Delft University of Technology: Delft, The Netherlands, 1980.
57. Leubner, I.H. Balanced nucleation and growth model for controlled crystal size distribution. *J. Disp. Sci. Technol.* **2002**, *23*, 577–590. [[CrossRef](#)]
58. Hanhoun, M.; Montastruc, L.; Azzaro-Pantel, C.; Biscans, B.; Freche, M.; Pibouleau, L. Simultaneous determination of nucleation and crystal growth kinetics of struvite using a thermodynamic modeling approach. *Chem. Eng. J.* **2013**, *215–216*, 903–912. [[CrossRef](#)]
59. Zumstein, R.C.; Rousseau, R.W. Growth rate dispersion by initial growth rate distributions and growth rate fluctuations. *AIChE J.* **1987**, *33*, 121–129. [[CrossRef](#)]
60. Buyevich, Y.A.; Alexandrov, D.V.; Mansurov, V.V. *Macrokinetics of Crystallization*; Begell House: New York, NY, USA, 2001.
61. Toropova, L.V.; Aseev, D.L.; Osipov, S.I.; Ivanov, A.A. Mathematical modeling of bulk and directional crystallization with the moving phase transition layer. *Math. Meth. Appl. Sci.* **2021**. [[CrossRef](#)]
62. Toropova, L.V.; Alexandrov, D.V.; Rettenmayr, M.; Liu, D. Microstructure and morphology of Si crystals grown in pure Si and Al-Si melts. *J. Phys. Condens. Matter* **2022**, *34*, 094002. [[CrossRef](#)] [[PubMed](#)]
63. Melikhov, I.V.; Belousova, T.Y.; Uludev, N.A.; Blyudev, N.T. Fluctuate the rate of growth of monocrystals. *Crystallography* **1974**, *19*, 1263–1268.
64. Shneidman, V. Early stages of Ostwald ripening. *Phys. Rev. E* **2013**, *88*, 010401. [[CrossRef](#)]
65. Caraballo, K.G.; Baird, J.K.; Ng, J.D. Comparison of the crystallization kinetics of canavalin and lysozyme. *Cryst. Growth Des.* **2006**, *6*, 874–888. [[CrossRef](#)]
66. Friedlander, S.K. *Smoke, Dust and Haze: Fundamentals of Aerosol Behaviour*; Wiley: New York, NY, USA, 1977.
67. Herlach, D.M. *Phase Transformations in Multicomponent Melts*; Wiley-VCH: Weinheim, Germany, 2008.
68. Slezov, V.V. *Kinetics of First-Order Phase Transitions*; Wiley: Weinheim, Germany, 2009.
69. Alexandrov, D.V. On the theory of fragmentation process with initial particle volume. *Commun. Theor. Phys.* **2017**, *68*, 269–271. [[CrossRef](#)]
70. Makoveeva, E.V.; Alexandrov, D.V. Effects of external heat/mass sources and withdrawal rates of crystals from a metastable liquid on the evolution of particulate assemblages. *Eur. Phys. J. Spec. Top.* **2019**, *228*, 25–34. [[CrossRef](#)]
71. Huppert, H.E.; Worster, M.G. Dynamic solidification of a binary melt. *Nature* **1985**, *314*, 703–707. [[CrossRef](#)]
72. Kerr, R.C.; Woods, A.W.; Worster, M.G.; Huppert, H.E. Solidification of an alloy cooled from above Part 1. Equilibrium growth. *J. Fluid Mech.* **1990**, *216*, 323–342. [[CrossRef](#)]
73. Peppin, S.S.L.; Aussillous, P.; Huppert, H.E.; Worster, M.G. Steady-state mushy layers: Experiments and theory. *J. Fluid Mech.* **2007**, *570*, 69–77. [[CrossRef](#)]
74. Peppin, S.S.L.; Huppert, H.E.; Worster, M.G. Steady-state solidification of aqueous ammonium chloride. *J. Fluid Mech.* **2008**, *599*, 465–476. [[CrossRef](#)]
75. Toropova, L.V.; Galenko, P.K.; Alexandrov, D.V.; Rettenmayr, M.; Kao, A.; Demange, G. Non-axisymmetric growth of dendrite with arbitrary symmetry in two and three dimensions: Sharp interface model vs. phase-field model. *Eur. Phys. J. Spec. Top.* **2020**, *229*, 2899–2909. [[CrossRef](#)]
76. Toropova, L.V. Shape functions for dendrite tips of SCN and Si. *Eur. Phys. J. Spec. Top.* **2022**, *231*, 1129–1133. [[CrossRef](#)]
77. Alexandrov, D.V.; Malygin, A.P. Analytical description of seawater crystallization in ice fissures and their influence on heat exchange between the ocean and the atmosphere. *Dokl. Earth Sci.* **2006**, *411*, 1407–1411. [[CrossRef](#)]

-
78. Toropova, L.V.; Alexandrov, D.V. Dynamical law of the phase interface motion in the presence of crystals nucleation. *Sci. Rep.* **2022**. [[CrossRef](#)]
 79. Alexandrov, D.V.; Bashkirtseva, I.A.; Ryashko, L.B. Nonlinear dynamics of mushy layers induced by external stochastic fluctuations. *Phil. Trans. R. Soc. A* **2018**, *376*, 20170216. [[CrossRef](#)]
 80. Nizovtseva, I.G.; Alexandrov, D.V. The effect of density changes on crystallization with a mushy layer. *Phil. Trans. R. Soc. A* **2020**, *378*, 20190248. [[CrossRef](#)]